Drug Design, Development and Therapy

Dovepress
Taylor & Francis Group

Open Access Full Text Article

ORIGINAL RESEARCH

Fragment Based Drug Discovery by Microscale Thermophoresis Targeting *Klebsiella pneumoniae* and *Escherichia coli* IspE

Danica J Walsh[1], Daan Willocx[1], Rawia Hamid[1,2], Mostafa M Hamed[1], Anna KH Hirsch[1,2]

[1]Department of Drug Design and Optimization, Helmholtz Institute for Pharmaceutical Research Saarland (HIPS) – Helmholtz Centre for Infection Research (HZI), Saarbrücken, 66123, Germany; [2]Department of Pharmacy, Saarland University, Saarbrücken, 66123, Germany

Correspondence: Anna KH Hirsch, Helmholtz Institute for Pharmaceutical Research (HIPS), Helmholtz Centre for Infection Research (HZI), Saarland University, Campus E8.1, Saarbrücken, 66123, Germany, Email Anna.hirsch@helmholtz-hips.de

Background: Antimicrobial drug discovery urgently requires innovative strategies to combat the growing threat of multidrug-resistant pathogens. The 2-*C*-methylerythritol 4-phosphate (MEP) pathway, essential in many pathogenic bacteria yet absent in humans, represents an attractive source of selective antibacterial targets. Within this pathway, the enzyme IspE is a promising candidate for inhibitor development.

Methods: We screened a halogen-enriched fragment library to identify inhibitors of IspE from *Klebsiella pneumoniae* and *Escherichia coli*. We validated our hits through biochemical assays, followed by structure–activity relationship (SAR) studies to optimize the fragments inhibitory activity. Mode-of-inhibition experiments were conducted to determine the mechanism of enzyme inhibition.

Results: Screening identified a fragment-like compound **1** and several additional hits that inhibited *K. pneumoniae* IspE and *E. coli* IspE at micromolar concentrations. SAR analysis generated optimized fragments with enhanced potency. Mode-of-inhibition assays revealed that these fragments act as competitive inhibitors with respect to the natural substrate, 4-diphosphocytidyl-2-*C*-methylerythritol (CDP-ME).

Conclusion: This newly identified fragment class provides a promising foundation for the development of IspE inhibitors. The findings highlight the utility of fragment-based screening approaches for discovering novel antimicrobial agents targeting the MEP pathway.

Keywords: IspE, fragment based drug discovery, *Klebsiella pneumoniae*, *Escherichia coli*, MEP pathway

Introduction

The 2-*C*-methyl-D-erythritol 4-phosphate (MEP) (Figure 1) pathway is a metabolic route that converts glyceraldehyde 3-phosphate (G3P) and pyruvate into the universal isoprenoid precursors isopentenyl diphosphate (IDP) and dimethylallyl diphosphate (DMADP). These precursors serve as the building blocks for the biosynthesis of isoprenoids, a large and diverse family of natural products that include compounds with vital functions such as vitamins, quinones, steroids, and secondary metabolites with essential cellular functions. The pathway proceeds through seven enzymatic steps catalyzed by the enzymes DXPS, DXR, IspD, IspE, IspF, IspG, and IspH. Each of these enzymes represents a potential antimicrobial drug target, as the pathway is indispensable in many pathogenic bacteria such as *Klebsiella pneumoniae* and *Escherichia coli* but absent in humans. The rapid development of antibiotic resistance in *K. pneumoniae* has led to a major health concern in recent years,[1,2] resulting in the urgent need for novel antimicrobial compounds endowed with a novel mechanism of action.

Despite the essential functions served by the downstream products of the MEP pathway, few inhibitors have been reported to date. Here, we focus on the fourth enzyme in the pathway, 4-diphosphocytidyl-2-*C*-methyl-D-erythritol kinase (IspE).

Previous studies have explored several compound classes as potential IspE inhibitors, but many have not translated successfully into whole-cell efficacy. The few reported IspE inhibitors bind to the CDP-Me binding pocket of IspE, typically at the cytidine binding site (Figure 2).[3–6] Compound classes **A** and **B** show promising inhibitory activity although, further optimization is needed due to lack of growth inhibition in whole cell assays. Against *E. coli* and *K. pneumoniae* IspE compound

Received: 18 June 2025
Accepted: 18 November 2025
Published: 18 December 2025

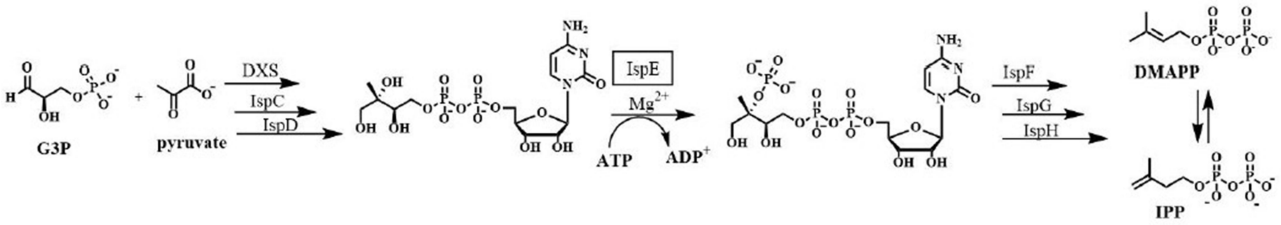

Figure 1 Representation of the 2-*C*-methyl-D-erythritol 4-phosphate pathway.

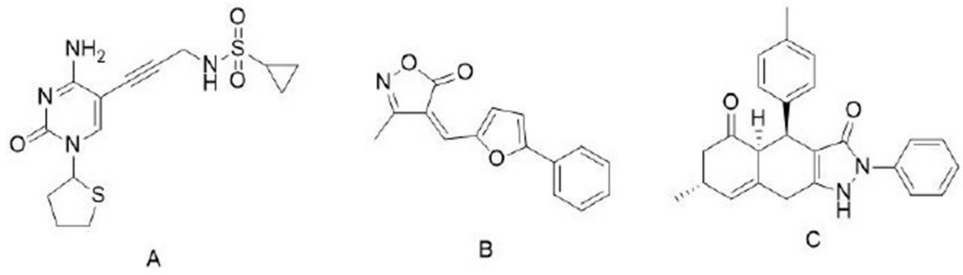

Figure 2 Examples of previously reported IspE inhibitors **A**, **B** and **C**.

A has an IC_{50} of 4.73 ± 1.19 μM and 7.7 ± 1.45 μM, respectively.[7] Compound **B** was also studied towards *E. coli* as well as *Yersinia pestis*, with recorded IC_{50} values of 5.5 μM and 6 μM, respectively. For instance, fragment and non–substrate-like inhibitors discovered through integrated in silico and in vitro high-throughput screening have demonstrated promising ligand efficiencies and favorable physicochemical profiles, yet still require substantial optimization before they can inhibit bacterial growth effectively.[8] More recent structure-based efforts across homologs—including *E. coli, K. pneumoniae*, and *Acinetobacter baumannii*—have illuminated subtle structural differences in substrate-binding pockets, particularly a more compact hydrophobic subpocket in *A. baumannii* IspE, suggesting that inhibitor design must account for species-specific variations.[9] Additionally, work on *Plasmodium falciparum* IspE has progressed from initial hits to a benzimidazole derivative (compound **19**) with measurable biochemical potency (IC_{50} ~53 μM) and encouraging whole-cell activity (IC_{50} ~0.82 μg/mL), representing a major step forward in bridging biochemical inhibition and cellular efficacy.[10] Finally, fragment-based virtual screening against *E. coli* IspE yielded a new class of inhibitors active against *P. aeruginosa* and *A. baumannii*, providing important insight into balancing enzyme selectivity and antimicrobial activity, though cytotoxicity remains a concern.[11] The evidence from other systems also informs our approach, highlighting how species-specific structural differences, the need to translate the enzyme-based potency to whole-cell efficacy, and managing off-target toxicity shape future inhibitor design and optimization.

This study aims at identifying fragments that bind to *K. pneumoniae* IspE (*Kp*IspE) without mimicking the cytidine moiety in order to expand the profile of available inhibitors. Fragment-based drug discovery (FBDD) is a widely used technique, which uses biophysical assays to detect the weak binding of "fragment molecules" to a specified target.[12] The detected fragment hits provide an efficient starting point for the generation of small-molecule inhibitors. The initial identification of fragments can be achieved through an array of different biophysical methods such as thermal shift, microscale thermophoresis (MST) surface plasmon resonance, and nuclear magnetic resonance spectroscopy.

Materials and Methods

Fragment Screening via MST

MST (Serial no. 201709-BR-N024, Monolith NT.115 Micro Scale Thermophoresis, NanoTemper Technologies GmbH) was performed according to the standard protocol from the manufacturer NanoTemper Technologies GmbH using the Monolith His-Tag Labeling Kit RED-tris-NTA 2nd Generation kit. The buffer used was HEPES (50 mM), $MgCl_2$ (5 mM) and Tween (0.05%) at pH 7.6 for all compounds. The protein concentration of 50 nM was used, and the ligand was tested at 2 mM. For each compound, only one concentration was tested, and compounds were compared to a standard that is

known to bind to *Kp*IspE with a K_d of 3.70 μM.[7] We chose ten compounds which were in the closest range to the standard, and determined their K_d value to confirm binding.

Microscale Thermophoresis for K_d Determination

The microscale thermophoresis (MST) (Serial no. 201709-BR-N024, Monolith NT.115 Micro Scale Thermophoresis, NanoTemper Technologies GmbH) was performed according to the standard protocol from the manufacturer NanoTemper Technologies GmbH using the Monolith His-Tag Labeling Kit RED-tris-NTA 2nd Generation kit. The buffer used was HEPES (50 mM), $MgCl_2$ (5 mM) and Tween (0.05%) at pH 7.6 for all other compounds. The protein concentration of 50 nM was used, and the ligand was tested at the highest soluble concentration, which was 2 mM for most of the compounds under the assay conditions. A 1:1 dilution of the ligand over 16 samples was performed using a stock of ligand stock (in water) diluted in HEPES buffer. Non-hydrophobic capillary tubes were used. A pretest to check for the labelling and compound fluorescence was performed before every sample, followed by a K_d determination. Each sample was measured after 15 min incubation time at RT and analyzed in MO Control version 1.6.

*Kp*IspE IC_{50} Assay

Assays were conducted in 384-well plates (Corning) with a transparent flat bottom. Assay buffer A (total volume, 30 μL) contained 200 mM Tris hydrochloride, pH 7.6 (containing 20 mM KCl, 10 mM $MgCl_2$, 10 mM DTT), 2 mM NADH, 2 mM phosphoenolpyruvic acid, 0.2 U of pyruvate kinase (PK), 0.2 U of lactate dehydrogenase (LDH) and 0.3 μM IspE *K. pneumoniae*. Assay buffer B contained 200 mM Tris hydrochloride, pH 7.6, 2 mM ATP and 0.6 mM CDP-ME. Compound stocks were made in DMSO (20mM) and further diluted in Tris HCl buffer to a concentration of 1.3 mM in 96-well plates, so that the starting concentration in the assay is 120 μM. Dilution series were performed with dilution step 1:2 and approximately covered the concentration range of 120 μM to 0.23 μM in the assay. The impact of the tested compounds on auxiliary enzymes in the photometric activity inhibition assay was tested as follows. Well 1 will serve as a blank and well 3 as a positive control. Assay buffer A (30 μL) was transferred into wells 1, 3, 5, 7 etc. Compound (6 μL) was added to wells 5, 7, 9, 11 etc. Tris HCl (30 μL) was transferred into well 1, while buffer B (30 μL) was transferred into wells 3, 5, 7, 9 etc, to start the reaction. The 384 well plate was centrifuged for 1 min. The reactions were monitored photometrically (room temperature) at 340 nm in a plate reader (SpectraMax5, Molecular Dynamics). Initial rate values were evaluated with a nonlinear regression method using the program Dynafit.[13] CDP-ME was used as starting substrate and was synthesized and purified as previously described.[14] *Kp*IspE was obtained and purified as previously reported.[15]

Competitive Binding Assay

Assays were conducted in 384-well plates (Corning) with a transparent flat bottom. Assay buffer A was made as in the above assay and buffer B was made the same as above with a range of amounts of either ATP (1400–43.75 mM) or CDP-ME (700–21.875 mM). Compound stocks were prepared in DMSO (20 mM) and further diluted in Tris HCl buffer to a concentration of 1.3 mM in 96 well plates, so that the starting concentration in the assay was 120 μM. A dilution series (1:2) of inhibitors in DMSO covered the concentration range of approximately 700–21 μM. The concentration of the inhibitor was kept constant as the concentration of CDP-ME or ATP was varied. Assay buffer B without CDP-ME (30 μL) was transferred into wells A and C 3, 5, 7, 9, 11, while 57.6 μL were added to column 1. To column 1 in rows A and C, 2.4 μL of 100 mM CDP-ME was added. Serial dilutions were done for columns 3, 5, 7, 9 and 11. Assay buffer B without ATP (30 μL) was transferred into wells E and G 3, 5, 7, 9, 11, while 56.6 μL were added to column 1. To column 1 in rows E and G, 3.4 μL of 100 mM ATP were added. Serial dilutions were done for columns 3, 5, 7, 9 and 11. Compound stocks were made same as in the above procedure so that starting concentrations are 120 μM–1.875 μM. To each well, 6 μL of the compound stock were added. Buffer A (30μL) were added to the reaction wells and read on Pherastar as with the same IC_{50} assay as stated above.

Chemistry

All reagents used for chemical synthesis and biological evaluation were purchased from commercial suppliers and used without further purification. The absence of further purification is due to the adequate purity of the starting compounds

used in synthesis. Screening chemicals, which were commercially available were purchased from Sigma Aldrich and were first evaluated via LCMS for purity of 95% or higher before use. All chemical yields refer to purified compounds and were not optimized. Reaction progress was monitored using TLC silica gel 60 F254 aluminum sheets, and visualization was accomplished by UV at 254 nm. Column chromatography was performed using the automated flash chromatography system CombiFlash® Rf (Teledyne Isco) equipped with RediSepRf silica columns. Preparative RP-HPLC was performed using an UltiMate 3000 Semi-Preparative System (Thermo Fisher Scientific) with nucleodur® C18 Gravity (250 mm × 10 mm, 5 μm) column. ^{1}H and ^{13}C NMR spectra were recorded as indicated on a Bruker Avance Neo 500 MHz (^{1}H, 500 MHz; 13C, 126 MHz) with prodigy cryoprobe system . Chemical shifts were recorded as δ values in ppm units and referenced against the residual solvent peak (DMSO-d6, δ = 2.50, 39.52). Splitting patterns describe apparent multiplicities and are designated as s (singlet), br s (broad singlet), d (doublet), dd (doublet of doublet), t (triplet), q (quartet), m (multiplet). Coupling constants (J) are given in hertz (Hz). Low resolution mass analytics and purity control of final compounds was carried outusing an Ultimate 3000-MSQ LCMS system (Thermo Fisher Scientific) consisting of a pump, an autosampler, MWD detector and an ESI quadrupole mass spectrometer. Purity of all compounds used in biological assays was ≥95%. Final products were dried under high vacuum. Further information can be found in the SI.

General Procedure for Amide Formation

To a microwave tube containing DMF and Cs_2CO_3, the appropriate nicotinic or picolinic acid and the respective amino compound were added. The resulting solution was stirred at 50°C overnight. Next water and EtOAc were added and the resulting solution was extracted (3x). The organic layer was washed with slightly acidic water (pH 4–5) (3x) followed by a wash with saturated aqueous NaCl solution. Subsequent, the combined organic layers were dried under reduced pressure, and the residues were washed (3x) with MeOH and diethyl ether. Final products were purified via column chromatography.

Results

In this study, we report the identification of a fragment hit with relatively good binding affinity for *Kp*IspE and anSAR study for optimization. Here, we used microscale thermophoresis (MST) to detect the binding of fragments to the *Kp*IspE protein. The MST screening procedure is detailed in the Supporting Information. FBDD typically begins with the screening of a low-molecular weight (<300 Da) library. For this, we used the halogen-enriched fragment library consisting of 198 compounds.[16] The MST screening resulted in fragment hit **1** with a K_d value of 213 μM and an IC_{50} value of 124.0 ± 1.13 μM. Compound **1** was an attractive starting point due to its potential for structural modification. To identify the structural features that are critical for *Kp*IspE inhibition and to optimize activity, we conducted an SAR study.

We started our SAR study by screening a series of commercially available analogues for inhibitory activity towards *Kp*IspE. The first set of compounds (**2**–**14**) kept the five-membered heterocyclic ring while incorporating variable substituents (Table 1). This was to determine the importance of the bromine as well as the pyrrole ring itself. The second set of compounds had a six-membered ring (Table 2) to determine if increasing ring size could enhance activity while keeping the single nitrogen atom.

First, we altered the functional groups on the pyrrole ring (**2**–**7**). In compounds **2**–**4**, we replaced the bromo with a chloro (**2**), nitro (**3**) and methyl (**4**) substituent. Although the bromine (**1**) was the most active, the nitro analogue **2** showed only a slight decrease in activity Compounds **5**, **6** and **7** have a methyl group in different positions. Of these methyl-substituted derivatives, only **7** with dimethyl groups demonstrated enhanced activity compared to **1**. Next, we altered the five-membered ring to determine the importance of the nitrogen atom in the pyrrole backbone. Compounds **8** and **9** have an oxygen and sulfur atom in place of the nitrogen, with only **8** showing activity towards *Kp*IspE. Compounds **9** and **10** also features a sulfur in place of the nitrogen atom although **10** is substituted with amino and chloro groups and is a methyl ester. Compound **10** also showed inhibitory activity towards *Kp*IspE, although lower than compound **1**. Compounds **11**–**14** explore a thiazole as the core structure. Thiazole was chosen because of its well-studied diverse range of biological activity.[17,18] Interestingly, the bromo-derivative (**11**) was the only inactive thiazole, while **12**, **13** and **14** displayed moderate activity.

Table 1 IC_{50} Values of Compounds **1–14** Determined Using the Coupled Spectrophotometric Assay with Purified *Klebsiella pneumoniae* IspE

#	Structure	*Kp*IspE IC_{50} (μM)	#	Structure	*Kp*IspE IC_{50} (μM)
1	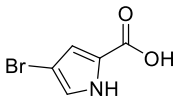	124.0 ± 1.1	**8**	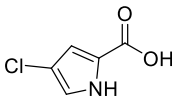	239.0 ± 8.8
2	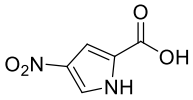	>500	**9**	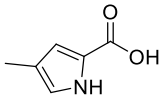	>500
3	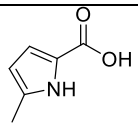	160.6 ± 8.3	**10**	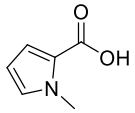	243.8 ± 9.5
4	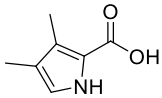	>500	**11**	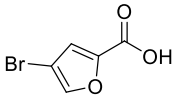	>500
5	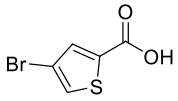	>500	**12**	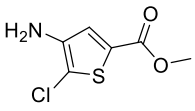	306.4 ± 1.2
6	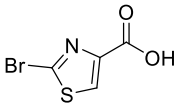	248.9 ± 7.8	**13**	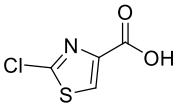	153.2 ± 8.1
7	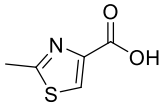	107.4 ± 11.6	**14**	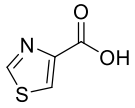	296.2 ± 13.8

Table 2 IC_{50} Values of Compounds **15–26** Determined Using the Coupled Spectrophotometric Assay with Purified *Klebsiella pneumoniae* IspE

#	Structure	*Kp*IspE IC_{50} (μM)	#	Structure	*Kp*IspE IC_{50} (μM)
15	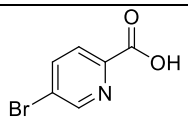	144.6 ± 4.5	**21**	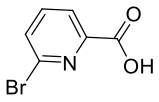	166.2 ± 6.2
16	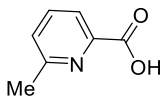	98.1 ± 4.8	**22**	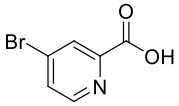	>500
17	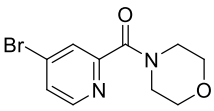	84.6 ± 4.9	**23**	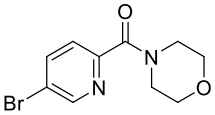	>500

(*Continued*)

https://doi.org/10.2147/DDDT.S538771

Table 2 (Continued).

#	Structure	*Kp*IspE IC_{50} (μM)	#	Structure	*Kp*IspE IC_{50} (μM)
18	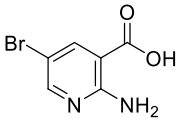	112.9 ± 1.2	**24**	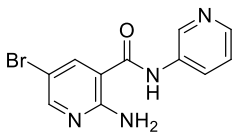	>500
19	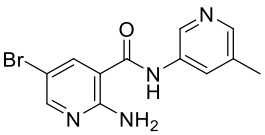	>500	**25**	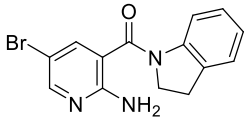	82.7 ± 1.6
20	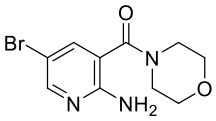	>500	**26**	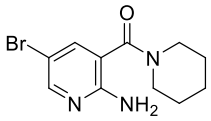	>500

Next, we focused on the pyridinyl ring (**15**–**26**). Compounds **19**, **20**, **22**–**26** were not commercially available and synthesized as follows (Scheme 1).[19] The appropriate picolinic or nicotinic acid was reacted with the corresponding primary or secondary amine at 50°C for 12 hours. We selected compounds **15**–**26** for this series because they maintain the nitrogen atom, while expanding the five-membered ring of **1** to a six-membered ring. Picolinic (**15**–**20**) and nicotinic acid derivatives (**21**–**26**) have also previously demonstrated antimicrobial activity.[20–22] The picolinic acid derivatives all showed good inhibitory activities with the exception of **19** and **20**, which had an IC_{50} value of >500 μM (Table 2). Compounds **16**–**18** were more active than compound **1**, with **17** being the most active picolinic acid derivative with an IC_{5o} value of 84.6 ± 4.9 μM.

The nicotinic acid **21** and the nicotinamide derivatives **22**–**26** possess a bromine in the 5-position and an amine in the 2-position. Surprisingly, only compounds **21** and **25** of these derivatives were active with **25** demonstrating an IC_{5o} value of 82.70 ± 1.6 μM (Table 2).

Several analogues showed decent *Kp*IspE inhibition, with IC_{50} values between 82.7 ± 1.6 and 306.4 ± 1.2 μM. Compound **7** was the only five-membered ring derivative more active than **1**, with an IC_{50} of 107.4 ± 11.6 μM, although several other six-membered ring derivatives were more active. The compounds, which showed enhanced activity compared to **1** were also evaluated for activity towards *E. coli* IspE (*Ec*IspE). The binding pocket of *Ec*IspE is structurally similar to that of *Kp*IspE, although *Ec*IspE has been studied to a greater extent.[15] The parent compound **1** (112.7 ± 1.91 μM) and compound **17** (83.1 ± 1.1 μM) showed inhibitory activity but surprisingly the other compounds showed no activity, with **17** being more active than **1** (Table S1).

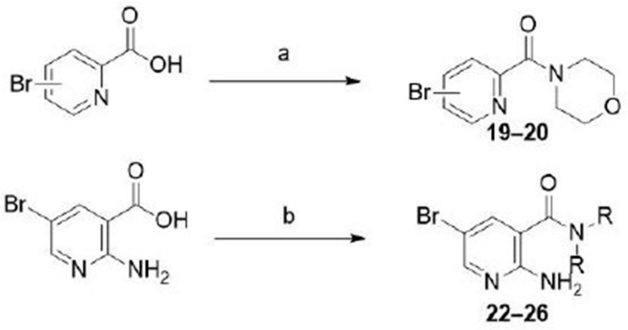

Scheme 1 General synthesis of compounds **19**–**20** and **22**–**26**. Reaction conditions for a and b: CsCO3, EtOAc, 50°C, 12 h. a) % yield 3–26%, b) % yield 15–44%.

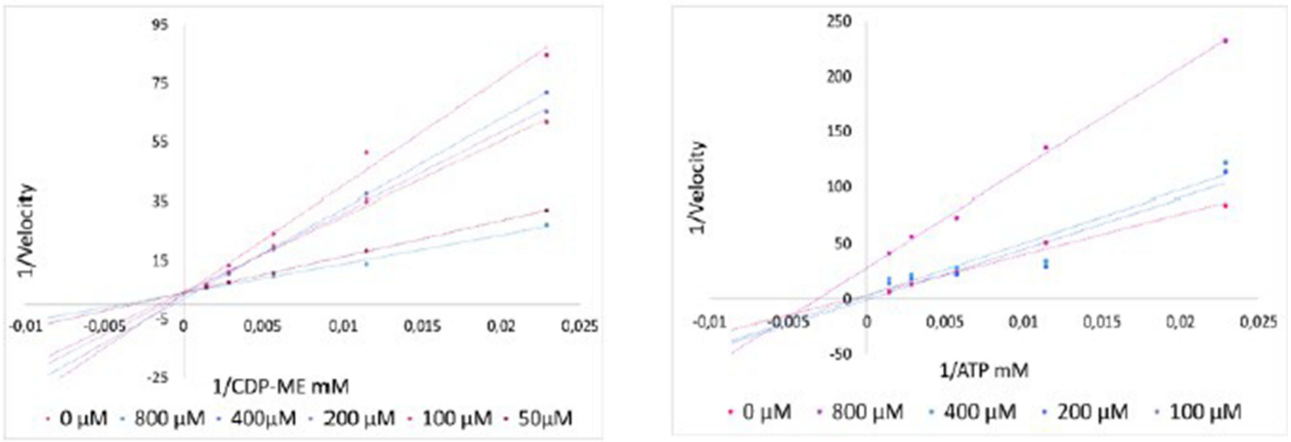

Figure 3 Lineweaver−Burk plots of both substrates, ATP and CDP-ME at varying concentrations of **1**. First CDP-ME was varied from 100–800 µM (left) and then the ATP was varied from 50–800 µM (right).

IspE catalyzes the ATP-dependent phosphorylation from CDP-ME to CDP-MEP, utilizing two substrates, ATP and CDP-ME. To understand the influence that compound **1** has on the enzymatic kinetics of ATP and CDP-ME substrates, we performed a mode-of-inhibition study. The results, plotted as Lineweaver−Burk plots (Figure 3), demonstrate that compound **1** is competitive with CDP-ME and non-competitive with ATP.

This finding indicates that compound **1** competes with CDP-ME for the active site of *Kp*IspE. Since affinity for the target is not the only aspect we are considering in the fragment-based drug discovery process, we also focused our attention on the physicochemical properties of the active compounds (Table 3). The cLogP, cLogS and cLogD scores

Table 3 The cLogP, cLogS and cLogD Scores as Well as Lipophilic Ligand-Efficiency (LLE) and IC_{50} Values for All Active Compounds

Compound	*Kp*IspE IC_{50}	cLogP	LLE	MW	cLogS	cLogD
1	124.0 ± 1.1	1.56	5.35	190	4.302	−1.653
3	160.6 ± 8.3	1.04	6.75	156.1	3.923	−1.852
6	248.9 ± 7.8	0.9845	5.62	125.1	5.19	−2.089
7	107.4 ± 11.6	1.58	5.39	139.2	4.093	−1.4
8	239.0 ± 8.8	1.76	4.86	191	4.82	−1.224
10	243.8 ± 9.5	1.71	4.90	191.6	3.695	0.9857
11	306.4 ± 1.2	1.24	5.27	163.6	4.889	−1.644
13	153.2 ± 8.1	1.1	5.74	143.2	4.988	−1.863
14	296.2 ± 13.8	0.7	5.85	129.1	5.434	−2.092
15	144.6 ± 4.5	1.3	5.52	202	4.225	−1.815
16	98.1 ± 4.8	1.3	5.68	202	4.225	−1.782
17	84.6 ± 4.9	0.9	6.16	137.1	5.824	−1.879
18	112.9 ± 1.2	1.3	5.62	202	4.225	−1.869
21	166.2 ± 6.2	1.0	5.83	2	3.946	−1.926
25	82.7 ± 1.6	0.2	6.93	1	3.623	0.01006

https://doi.org/10.2147/DDDT.S538771

were calculated with StarDrop version: 7.0.1.29911, and the lipophilic ligand-efficiency (LLE) values were calculated using the predicted cLogP and IC_{50} values (LLE = pIC_{50} − cLogP).

In the present study, we used the fragment-based drug design approach to identify promising IspE inhibitors. Through the screening of a small, halogen-enriched fragment library via MST, compound **1** was identified. Optimization of this fragment was successfully carried out via the addition of two methyl groups (**7**) as well as the expansion of the five− to a six−membered ring (**16**, **17** and **25**). These four compounds are all within the ideal range for the predicted LLE (~5−7). Regarding these factors and the improved *Kp*IspE IC_{50} of **17** compared to **1**, we regard this as our best fragment overall. Additionally, **17** showed enhanced activity towards both *Kp* and *Ec*IspE, which can be furtheroptimized during the fragment-growing processes. It was also shown that **1** is competitive with CDP-ME but non-competitive with ATP, this fragment is also being considered for further optimization. These results have set the basis for the further development of more active *K. pneumoniae* and *E. coli* IspE inhibitors. As a next step in fragment-based drug design, these initial hits can be advanced through fragment growing and elaboration strategies to improve binding affinity, selectivity, and physicochemical properties. Such optimization efforts will be crucial for translating these early-stage fragments into potent, drug-like inhibitors with antibacterial activity in whole-cell assays.

Acknowledgments

We would like to acknowledge Prof. Frank Boeckler from the University of Tübingen for providing the halogen-enriched fragment library. The authors would like to thank the technicians at HIPS for technical support, specifically Simone Amann, Jeannine Jung and Jannine Seelbach. The authors would also like to recognize Dr Boris Illarionov and Prof. Markus Fischer at Hamburg School of Food Science, Institute of Food Chemistry for their contribution of reagents necessary for biological assays. D.J.W. received funding from the Marie Skłodowska-Curie Action Postdoctoral Fellowship, Grant agreement number 101103471. D.W. received funding from the European Union's Horizon 2020 research and innovation program under the Marie Skłodowska-Curie, grant agreement No 860816. MepAnti.

Author Contributions

All authors made a significant contribution to the work reported, whether in the conception, study design, execution, acquisition of data, analysis and interpretation, or in all these areas; took part in drafting, revising or critically reviewing the article; gave final approval of the version to be published; have agreed on the journal to which the article has been submitted; and agree to be accountable for all aspects of the work. All authors have given approval of the final version.

Disclosure

The authors report no conflicts of interest in this work.

References

1. Ballén V, Gabasa Y, Ratia C, Ortega R, Tejero M, Soto S. Antibiotic resistance and virulence profiles of *Klebsiella pneumoniae* strains isolated from different clinical sources. *Front Cell Infect Microbiol*. 2021;11. doi:10.3389/fcimb.2021.738223
2. Nirwati H, Sinanjung K, Fahrunissa F, et al. Biofilm formation and antibiotic resistance of *Klebsiella pneumoniae* isolated from clinical samples in a tertiary care hospital, Klaten, Indonesia. *BMC Proc*. 2019;13(Suppl 11):20. doi:10.1186/s12919-019-0176-7
3. Hirsch AKH, Alphey MS, Lauw S, et al. Inhibitors of the kinase IspE: structure–activity relationships and co-crystal structure analysis. *Org Biomol Chem*. 2008;6(15):2719–2730. doi:10.1039/b804375b
4. Crane CM, Hirsch AKH, Alphey MS, et al. Synthesis and characterization of cytidine derivatives that inhibit the kinase IspE of the non-mevalonate pathway for isoprenoid biosynthesis. *ChemMedChem*. 2008;3(1):91–101. doi:10.1002/cmdc.200700208
5. Tang M, Odejinmi SI, Allette YM, Vankayalapati H, Lai K. Identification of novel small molecule inhibitors of 4-diphosphocytidyl-2-C-methyl-d-erythritol (CDP-ME) kinase of Gram-negative bacteria. *Bioorg Med Chem*. 2011;19(19):5886–5895. doi:10.1016/j.bmc.2011.08.012
6. Choi S-R, Narayanasamy P. Investigating novel IspE inhibitors of the MEP pathway in mycobacterium. *Microorganisms*. 2024;12(1):18. doi:10.3390/microorganisms12010018
7. Hirsch AKH, Lauw S, Gersbach P, et al. Nonphosphate inhibitors of IspE protein, a kinase in the non-mevalonate pathway for Isoprenoid biosynthesis and a potential target for antimalarial therapy. *ChemMedChem*. 2007;2(6):806–810. doi:10.1002/cmdc.200700014
8. Tidten-Luksch N, Grimaldi R, Torrie LS, Frearson JA, Hunter WN, Brenk R. IspE inhibitors identified by a combination of in silico and in vitro high-throughput screening. *PLoS One*. 2012;7(4):e35792. doi:10.1371/journal.pone.0035792
9. Hamid R, Walsh DJ, Diamanti E, et al. IspE kinase as an anti-infective target: role of a hydrophobic pocket in inhibitor binding. *Structure*. 2024;32(12):2390–2398.e2. doi:10.1016/j.str.2024.10.009

10. Diamanti E, Steinbach AM, de Carvalho LP, et al. Targeting the Plasmodium falciparum IspE enzyme. *ACS Omega*. 2024;9(44):44465–44473. doi:10.1021/acsomega.4c06038
11. Ropponen HK, Diamanti E, Johannsen S, et al. Exploring the translational gap of a novel class of Escherichia coli IspE inhibitors. *ChemMedChem*. 2023;18(19):e202300346. doi:10.1002/cmdc.202300346
12. Erlanson DA. *Introduction to Fragment-Based Drug Discovery. In Fragment-Based Drug Discovery and X-Ray Crystallography*. Davies TG, Hyvönen M, Eds.. Berlin, Heidelberg: Springer Berlin Heidelberg; 2012:1–32.
13. Kuzmič P. Program DYNAFIT for the analysis of enzyme kinetic data: application to HIV proteinase. *Anal Biochem*. 1996;237(2):260–273. doi:10.1006/abio.1996.0238
14. Honold A, Lettl C, Schindele F, et al. Inhibitors of the bifunctional 2-C-Methyl-d-erythritol 4-phosphate Cytidylyl transferase/2-C-Methyl-d-erythritol-2,4-cyclopyrophosphate synthase (IspDF) of Helicobacter pylori. *Helvetica Chim Acta*. 2019;102(3):e1800228. doi:10.1002/hlca.201800228
15. Hamid R, Walsh DJ, Diamanti E, et al. IspE kinase as an anti-infective target: role of a hydrophobic pocket in inhibitor binding. *Structure*. 2024 32;2390–2398.e2 doi:10.1016/j.str.2024.10.009.
16. Zimmermann MO, Lange A, Wilcken R, et al. Halogen-enriched fragment libraries as chemical probes for harnessing halogen bonding in fragment-based lead discovery. *Future Med Chem*. 2014;6(6):617–639. doi:10.4155/fmc.14.20
17. Kashyap SJ, Garg VK, Sharma PK, Kumar N, Dudhe R, Gupta JK. Thiazoles: having diverse biological activities. *Med Chem Res*. 2012;21(8):2123–2132. doi:10.1007/s00044-011-9685-2
18. Petrou A, Fesatidou M, Geronikaki A. Thiazole Ring—A Biologically Active Scaffold. *Molecules*. 2021;26(11):3166. doi:10.3390/molecules26113166
19. Willocx D, D'Auria L, Walsh D, et al. Fragment discovery by X-Ray crystallographic screening targeting the CTP binding site of Pseudomonas aeruginosa IspD. *Angew Chem Int Ed*. 2025;64:e202414615. doi:10.1002/anie.202414615
20. Morjan RY, Mkadmh AM, Beadham I, et al. Antibacterial activities of novel nicotinic acid hydrazides and their conversion into N-acetyl-1,3,4-oxadiazoles. *Bioorg Med Chem Lett*. 2014;24(24):5796–5800. doi:10.1016/j.bmcl.2014.10.029
21. Acid P. Antimicrobial activity of picolinic acid; 2013.
22. Marković BA, Marinković A, Stanković JA, et al. Synthesis and antimicrobial activity of newly synthesized nicotinamides. *Pharmaceutics*. 2024;16:8. doi:10.3390/pharmaceutics16081084